

Thermodynamics and kinetics of ion translocation in the human wild-type and E-1'A $\alpha 7$ nicotinic receptor

G. COTTONE⁽¹⁾, L. CHIODO⁽²⁾ and L. MARAGLIANO⁽³⁾⁽⁴⁾

⁽¹⁾ *Dipartimento di Fisica e Chimica Emilio Segrè, Università di Palermo
Viale delle Scienze 17, 90123 Palermo, Italy*

⁽²⁾ *Department of Engineering, Campus Bio-Medico University of Rome
Via Á. del Portillo 21, 00128 Rome, Italy*

⁽³⁾ *Department of Life and Environmental Sciences, Marche Polytechnic University
Via Brecce Bianche, 60131, Ancona, Italy*

⁽⁴⁾ *Center for Synaptic Neuroscience and Technology (NSYN@UniGe), Istituto Italiano di
Tecnologia - Largo Rosanna Benzi, 10, 16132 Genova, Italy*

received 11 January 2021

Summary. — We use an all-atom model of the human nicotinic acetylcholine receptor $\alpha 7$ in a conductive conformation, to provide the first available mapping of the potential of mean force for the ion translocation across the channel. The modeling is based on MD simulations combined with the milestoning method with Voronoi tessellation. The quality of the protein model and description is confirmed by the agreement with experimental data for proteins of the same family. The specific mutation E-1'A at the cytoplasmatic filter is here shown to strongly affect both sodium and chloride permeation, leading to a complete inversion of selectivity.

1. – Introduction

The $\alpha 7$ nicotinic acetylcholine receptor (nAChR) is a ligand-gated ion channel (LGIC) widely expressed in the human brain, and related to schizophrenia and Alzheimer's disease [1]. In recent years, a growing number of LGICs structures become available (for a review see in ref. [2]). No high-resolution structure of the full-length human $\alpha 7$ structure has been reported until the last months, when cryo-em structures have been deposited in three major conformational states of the gating cycle, *i.e.* resting, activated, and desensitized [3, 4]. Meanwhile, due to its pharmacological relevance, a strong modelling effort has been devoted to obtain reliable models of this channel [5]. Within this framework, we provided an all-atom model of $\alpha 7$, comprising both the transmembrane domain (TMD) and the ligand binding domain (LBD) [2, 6-9]. Structural annotation allowed us to associate different conformations to different functional states. A comparison with

the recent experimental structures of the channels today confirms the accuracy of our models.

Functional annotation of LGICs models could be accomplished by investigating the ion translocation process through the channel. This is a rare event associated with crossing high free energy (FE) barriers encountered by the ion in its path from the LDB/TMD interface towards the intracellular side. Therefore in the past enhanced sampling techniques have been exploited to reconstruct the FE landscape underlying the process in LGICs channels, including nAChRs, with different methods and approximations, by limiting the calculations to the TMD or with implicit description of other regions of the system (see refs. in [2]). Here we present an all-atoms study of ion permeation across the full-length (TMD+LBD) human $\alpha 7$ channel model, in a lipid bilayer and with explicit water, both in wild-type (wt) and in the E-1'A mutant. The single-ion PMF and the ion translocation kinetics are reconstructed by using the milestoning method [10] with Voronoi tessellation [11,12]. Details on the calculations are fully reported in ref. [2].

The milestoning approach provides at the same time the FE barriers to ion translocation and the characteristic time (mean first passage time, MFPT) of the full process [13-15]. Results here obtained are consistent with the experimentally known cationic nature of the wt channel, while it is shown how the E-1'A mutation affects the ion permeation process for both ions, in particular causing an inversion of selectivity.

2. – Results and discussion

The wt $\alpha 7$ single ion PMF profiles are shown in fig. 1. Starting from the cytoplasmatic (intracellular) side, the sodium profile exhibits a deep minimum in correspondence of the E-1'-S2' rings. A barrier (2 kcal/mol) is located in the middle of the pore at the hydrophobic girdle (HG, L9'-L16'), indicating that the channel is indeed in a cation conductive conformation. The chloride profile presents the largest barrier (6 kcal/mol) at the intracellular side of the channel, mostly due to the E-1' residues, indicating that this ring plays the dominant role in ion selection. A secondary peak of about 4 kcal/mol

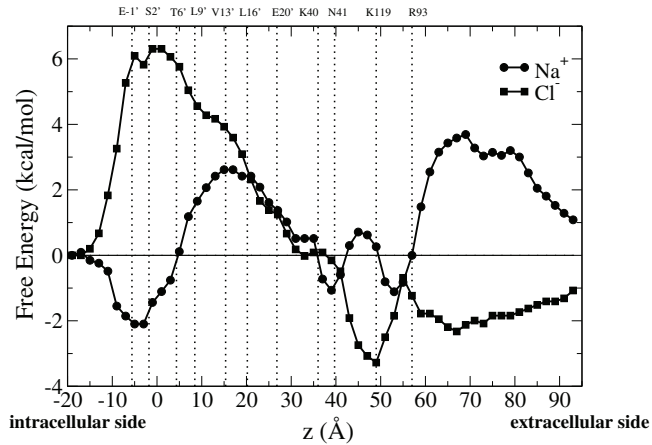


Fig. 1. – PMF for the ion permeation. The curves are shifted along the y -axis so that their values matches at the intracellular side. Positions of M2 pore-lining residues and of key residues in the LBD are indicated with dotted lines. All key residues are labeled at the top of the graph.

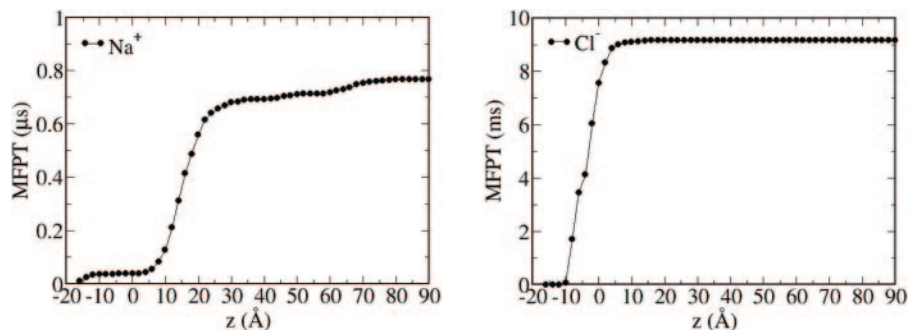


Fig. 2. – Mean first passage times from all milestones from the extracellular to the intracellular side milestone. Left panel: sodium; right panel: chloride.

is located at the HG, in agreement with the literature [16,17]. An estimate of the single-channel maximum conductance [18] based on the TMD portion of the PMF profiles gives 0.17 pS for chloride and 1.7 pS for sodium. The result is consistent with the preferential selectivity of wt $\alpha 7$ for cations. In the LBD sodium and chloride PMF profiles are symmetric, and arise from repulsion/attraction of pore facing charged/polar residue rings, respectively. The small barrier for sodium in the range 40–60 Å arises from arginine/lysine and polar asparagine rings facing the pore, which however provide a deep minimum at -4 kcal/mol for chloride. The sodium profile presents another wide barrier in the range 60–90 Å (4 kcal/mol); in this range a shallow minimum (2 kcal/mol) is observed for the chloride. Milestoning MFPTs for ion permeation from the extracellular to the intracellular side (from $+90$ Å down to -20 Å, see fig. 1) are shown in fig. 2. The MFPT to traverse the full channel is smaller for sodium than chloride (0.784 μ s and 9.165 ms, respectively), consistent with the cationic nature of wt $\alpha 7$. Moreover, results indicate that the FE barriers in the TMD play the major role in ion permeation, as the MFPTs are only slightly reduced along the LBD.

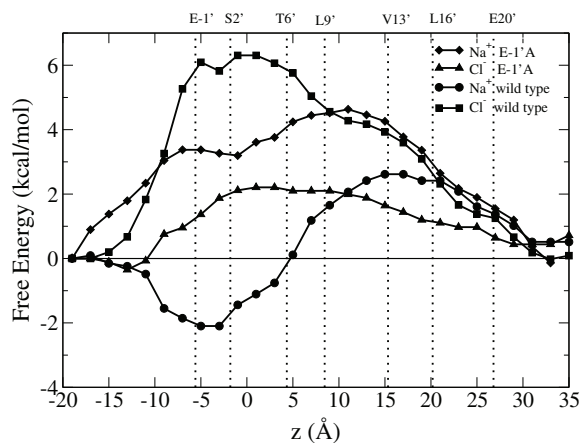


Fig. 3. – Potential of mean force for the permeation of sodium and chloride through the TMD in the E-1'A mutant compared with the wt channel. Positions of M2 pore-lining residues are indicated with black dotted lines and labeled at the top of the graph.

The single ion PMF profiles in the TMD of the mutant are shown in fig. 3. The effect of neutralizing the E-1' ring with alanines is very different for the two ions, and in the opposite direction. The kinetic trap for the sodium at E-1'-S2' disappears, while the barrier at the HG increases from 2 kcal/mol to 4 kcal/mol. On the contrary, the chloride PMF exhibits a reduction of about 4 kcal/mol with respect to the wt profile in the same region. The single-channel conductances are 3.3 pS for sodium and 45 pS for chloride. Compared with the wt value, it seems that the selectivity has been inverted. Indeed, the MFPTs from the TMD/LBD interface milestone are 1 μ s for sodium and only 36 ns for chloride. Similar results have been found by mutating other LGICs sharing GLU at the -1' position (see, *e.g.*, in [19]). In our case, a careful analysis reveals that chloride interactions with polar rings at the HG assist the ion translocation leading to a lower FE path through the hydrophobic region.

REFERENCES

- [1] CHANGEUX J. P., *J. Biol. Chem.*, **287** (2012) 40207.
- [2] COTTONE G., CHIODO L. and MARAGLIANO L., *J. Chem. Inf. Model.*, **60** (2020) 5045.
- [3] NOVIELLO C.M., GHARPURE A., MUKHTASIMOVA N. , CABUCO R., BAXTER L., BOREK D., SINE S. M. and HIBBS R. E., *Cell*, **184** (2021) 2121.
- [4] ZHAO G., LIU S., ZHOU Y., ZHANG M., CHEN H., XU H. E., SUN D., LIU L. and TIAN C., *Cell Res.*, **31** (2021) 713.
- [5] GULSEVIN A., PAPKE R.L. and HORENSTEIN N., *Mini Rev. Med. Chem.*, **20** (2020) 841.
- [6] CHIODO L., MALLIAVIN T. E., MARAGLIANO L., COTTONE G. and CICCOTTI G., *PLoS ONE*, **10** (2015) e0133011.
- [7] CHIODO L., MALLIAVIN T. E., MARAGLIANO L. and COTTONE G., *Biophys. Chem.*, **229** (2017) 99.
- [8] CHIODO L., MALLIAVIN T. E., GIUFFRIDA S., MARAGLIANO L. and COTTONE G., *J. Chem. Inf. Model.*, **11** (2018) 2278.
- [9] MOHAMMAD HOSSEINI NAVEH Z., MALLIAVIN T. E., MARAGLIANO L., COTTONE G. and CICCOTTI G., *PLoS ONE*, **9** (2014) e88555.
- [10] FARADJIAN A. K. and ELBER R., *J. Chem. Phys.*, **120** (2004) 10880.
- [11] VANDEN-EIJNDEN E. and VENTUROLI M., *J. Chem. Phys.*, **130** (2009) 194101.
- [12] MARAGLIANO L., VANDEN-EIJNDEN E. and ROUX B., *J. Chem. Theory Comput.*, **5** (2009) 2589.
- [13] YU T.Q, LAPELOSA M., VANDEN-EIJNDEN E. and ABRAMS C. F., *J. Am. Chem. Soc.*, **137** (2015) 3041.
- [14] ALBERINI G., BENFENATI F. and MARAGLIANO L., *J. Phys. Chem. B*, **22** (2018) 10783.
- [15] ALBERINI G., BENFENATI F. and MARAGLIANO L., *J. Chem. Inf. Model.*, **61** (2021) 1354.
- [16] CHENG M. H., COALSON R. D. and TANG P., *J. Am. Chem. Soc.*, **132** (2010) 16442.
- [17] IVANOV I., CHENG X., SINE S. M. and MCCAMMON J. A., *J. Am. Chem. Soc.*, **129** (2007) 8217.
- [18] BECKSTEIN O. and SANSOM M. S. P., *Phys. Biol.*, **3** (2006) 147.
- [19] THOMPSON A. J. and LUMMIS S. C., *Br. J. Pharmacol.*, **140** (2003) 359.